

# PRECISE CHARGE MEASUREMENT FOR LASER PLASMA ACCELERATORS \*

K. Nakamura, A. J. Gonsalves, C. Lin, T. Sokollik, S. Shiraishi, J. van Tilborg, J. Osterhoff<sup>†</sup>,  
R. J. Donahue, D. E. Rodgers, A. R. Smith, W. E. Byrne, and W. P. Leemans<sup>‡</sup>  
Lawrence Berkeley National Laboratory, Berkeley, CA 94720, USA

## Abstract

Cross-calibrations of charge diagnostics are conducted to verify their validity for measuring electron beams produced by laser plasma accelerators (LPAs). Employed diagnostics are a scintillating screen, activation based measurement, and integrating current transformer. The diagnostics agreed within  $\pm 8\%$ , showing that they can provide accurate charge measurements for LPAs provided they are used properly.

## INTRODUCTION

Laser plasma accelerators (LPAs) [1] have shown remarkable progress over the past decade. In 2006, the production of GeV electron beams was demonstrated in just a few centimeters [2, 3], using a discharge capillary based guiding structure [4]. This progress is making LPAs attractive as a driver for a light source that produces electromagnetic radiation ranging from THz [5] to x-ray [6].

A precise measurement of electron beam (e-beam) charge is essential for any kind of accelerator. Numerous technologies have been developed for conventional radio-frequency accelerators (RFAs) such as Faraday cups and integrating current transformers (ICTs) [7]. Since an LPA can provide e-beams with a wide range of energy spreads (from 1 % level to 100 %) and angular divergence, various techniques including previously mentioned technologies have been employed, e.g., surface barrier detectors [8], scintillating fibers [9], activation based measurements [10], imaging plates (IPs) [6], and scintillating screens with cameras [8]. Scintillating screens and IPs are now widely used as they allow large areas to be imaged with reasonable sensitivity and cost.

The light yield from the scintillating screens has been experimentally calibrated against ICTs by using e-beams from RFA with 3 - 8 MeV electron energy [11] and 40 MeV electron energy [12]. By using broadband electron beams from an LPA, sensitivity for 1 to 80 MeV electrons was experimentally calibrated against IPs [13]. For higher energies, the screens were cross-calibrated with an ICT for up to the electron energy of 1.5 GeV [14].

Faraday cups and ICTs have been used as reliable charge diagnostics in the RFA community [7, 15]. Since Faraday cups have to physically capture electrons, their size can be fairly large to stop GeV electrons. In contrast, ICTs are

non-destructive, energy independent and compact. Despite all of the favorable features of the ICT for LPA, its use for LPA produced e-beams has been questioned in recent studies. It was reported in Ref. [11] that the ICT overestimated the e-beam charge by more than an order of magnitude compared to the measurement based on the RFA-calibrated scintillating screen, and the source of discrepancy was attributed to the electromagnetic pulse (EMP) from the laser-plasma interaction. Another cross-calibration using LPA produced e-beams was done in Ref. [16], where it was reported that an ICT overestimated the charge by a factor of about 3 - 4 compared to the IP based charge measurements. Both studies indicated that further cross-calibrations and detailed investigations were necessary regarding the use of the ICT in a harsh laser-plasma environment.

In this paper, a comprehensive study of charge diagnostics for LPAs was performed using an ICT, Lanex Fast screen (Lanex), and activation based measurement. The activation based measurement is intrinsically RF noise tolerant and independent of the e-beam intensity. Therefore, it can provide an accurate reference for LPA produced e-beams. The Lanex that was calibrated by RFA produced e-beams was benchmarked against the activation based measurement using LPA produced e-beams. Also the ICT was cross-calibrated against Lanex using LPA produced e-beams. The results show that the Lanex and ICT can be accurate diagnostics for an LPA.

## EXPERIMENTAL SETUP

Cross-calibrations were conducted by using LPA produced e-beams at the LOASIS facility, LBNL. The laser that was utilized was a short pulse, high peak power and high repetition rate (10 Hz) Ti:Al<sub>2</sub>O<sub>3</sub> laser system. The laser beam was focused by an off-axis parabolic mirror, providing a focal spot size  $r_0 \simeq 23 \mu\text{m}$  with Strehl ratio of 0.9. Here, a Gaussian transverse profile of  $I = I_0 \exp(-2r^2/r_0^2)$  is assumed. Full energy and optimum compression gives  $P = 31 \text{ TW}$  ( $\tau_{in} \simeq 40 \text{ fs}$  FWHM), calculated peak intensity  $I_0 = 2P/\pi r_0^2 \simeq 3.4 \times 10^{18} \text{ W/cm}^2$ , and a normalized vector potential  $a_0 \simeq 8.6 \times 10^{-10} \lambda[\mu\text{m}] I^{1/2} [\text{W/cm}^2] \simeq 1.3$ .

The schematic drawing of the setup is shown in Fig. 1. The laser pulse was focused onto a supersonic gas jet. For the cross-calibrations, the magnet was turned off to send e-beams to charge diagnostics located further downstream. The laser pulse was reflected by the aluminum coated mylar foil toward the laser beam dump, and only e-beams went through following vacuum tubes.

\* Work supported by DOE grant DE-AC02-05CH11231

<sup>†</sup> Currently at University of Hamburg and DESY

<sup>‡</sup> WPLeemans@lbl.gov

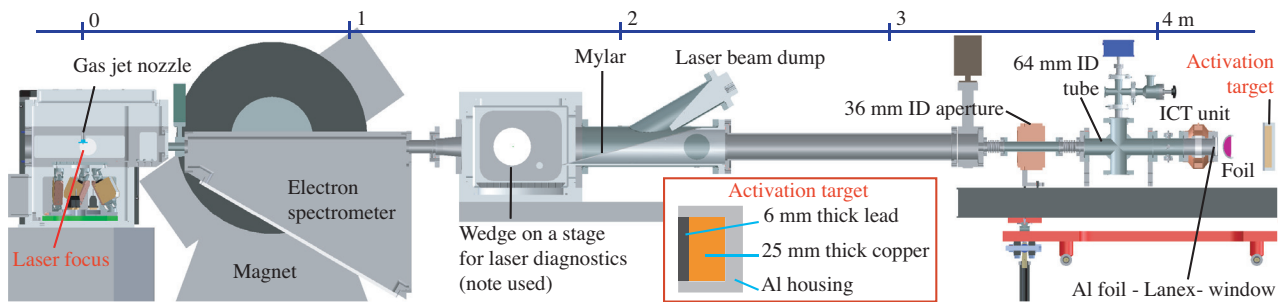


Figure 1: Setup for the charge cross-calibrations with LPA produced e-beams. Shown in the inset is the activation target.

An aperture with a 36 mm inner diameter was installed about 3.6 m away from the interaction point. The identical ICT unit described in Ref. [14] followed by the borosilicate vacuum window, was installed at the end of the vacuum tube. The Lanex Fast Front was placed on the window inside of the vacuum tube, covered by a  $\simeq 40 \mu\text{m}$  thick aluminum foil.

The light from Lanex was observed by a CCD camera through the reflection of an aluminum coated  $5 \mu\text{m}$  thick pellicle foil installed in the outside of the vacuum tube. For the activation measurement, the target was placed behind of the pellicle foil. The target consisted of 6 mm thick lead as a  $\gamma$ -ray generator followed by the 25 mm thick copper as an activation material, and is illustrated in Fig. 1 inset.

## RESULTS AND DISCUSSIONS

### Lanex – Activation Cross-Calibration

The activation based charge diagnostic was used as follows. The target material was irradiated by e-beams for  $\simeq 1$  hour. After the irradiation, the target was transferred to an ultra-low background counting facility at LBNL, where  $\gamma$ -ray spectroscopy was conducted. Based on the  $\gamma$ -ray spectroscopy results, the activity in terms of the average production rate  $R_{exp}$  (atoms/minute) for a specific isotope was calculated. In order to estimate the charge, a Monte-Carlo simulation was carried out to calculate the yield of an isotope for a unit charge with a certain e-beam energy spectrum  $Y_{sim}$  (atoms/electron). The e-beam energy spectrum was separately measured during the experiments. The number of electrons per minute irradiated to the target  $\bar{N}_e$  was obtained from  $\bar{N}_e = R_{exp}/Y_{sim}$ . As the result, the activation method can provide the time-averaged charge for e-beams with known energy spectrum.

The laser pulse was focused onto the hydrogen jet, and the peak plasma density was measured to be  $\sim 1.9 \times 10^{19}/\text{cm}^3$ . The e-beam energy spectra were measured by a single shot magnetic electron spectrometer [17] before sending the e-beam to charge diagnostics, and reproducible broadband e-beams up to 250 MeV were observed. The reference e-beam spectrum was obtained by averaging 50 shots. After the reference spectrum was obtained, a total of 2700 shots was incident onto the target in 60 minutes.

During the activation, the e-beam charge was simultaneously measured by the Lanex. The averaged number of electrons in a minute measured by the Lanex  $\bar{N}_{eLanx} = (10.3 \pm 0.4) \times 10^9$  electrons/minute.

After the irradiation, the target was transferred to the counting facility, and  $\gamma$ -ray spectroscopy was conducted by using a p-type HPGe detector. The 1345 keV photons from  $^{64}\text{Cu}$  decay (half life time 12.7 hour) was used to determine the yield of the isotope. Assuming the constant production rate during the irradiation, the average production rate  $R_{exp}$  was measured to be  $(9.79 \pm 0.59) \times 10^6$  atoms/minute, where the error was given by the  $\pm 1\sigma$  (standard deviation).

A Monte-Carlo simulation was carried out to estimate isotope production based on the e-beam reference spectrum [18]. An axisymmetric, three-dimensional distribution of the isotope production was calculated. In the simulation, energy losses of electrons due to the interactions with the foil, Lanex, vacuum window, and air were included. The simulated yield of the isotope  $Y_{sim}$  was  $1.02 \times 10^{-3}$  atoms/electron, giving  $\bar{N}_{eAct} = R_{exp}/Y_{sim} = (9.6 \pm 0.6) \times 10^9$  electrons/minute. The charge measured by the activation based measurement  $\bar{N}_{eAct} = (9.6 \pm 0.6) \times 10^9$  and the Lanex measurement  $\bar{N}_{eLanx} = (10.3 \pm 0.4) \times 10^9$  agreed with each other within the error of each measurement.

### Lanex – ICT Cross-Calibration

For the Lanex – ICT Cross-calibration, the laser pulses were focused onto the downstream edge of a gas jet comprised of 99% helium and 1% nitrogen. The gas jet backing pressure was varied to change charge yield from the LPA. The peak plasma density was measured by transverse interferometry, and was found to be from  $4$  to  $10 \times 10^{18}/\text{cm}^3$ , and the longitudinal plasma length was about 0.5 mm. Reproducible e-beams up to 60 MeV were observed. Higher plasma density resulted in producing e-beams with higher charge and broader spectra.

A total of 320 shots was recorded while varying the plasma density, and e-beams with charge up to 16 pC were observed. Shown in Fig. 2 is the charge measured by the Lanex versus the charge measured by the ICT. A linear fit performed on the data set indicated that the Lanex measured 8% lower charge with the offset of -1 pC. The two

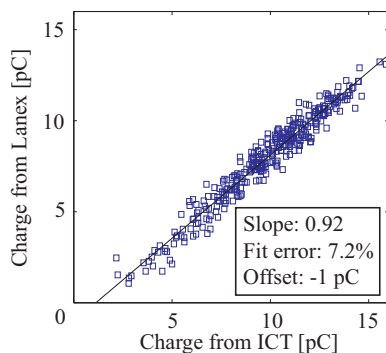


Figure 2: Lanex versus ICT.

diagnostics showed good agreement considering the fit error of 7.2%. The 1 pC of negative offset was probably due to the sensitivity of the CCD camera.

### Discussions

As shown above, the ICT can measure the LPA produced e-beam charge accurately, while previous works showed that the ICT overestimated the charge more than an order of magnitude. The excellent agreement we observed can be explained by the special attentions paid to the following three possible noise sources of the ICT measurement: (1) EMP from the laser plasma interaction, (2) direct particle/radiation hit on the ICT, and (3) low energy electrons.

There were two kinds of EMP noises observed, one was directly on the scope, and the other was on the cable and/or the ICT. The noise on the oscilloscope was separated from the signal in the time domain by extending the cable length. To minimize the noise on the cable, well-shielded cables (Helix FSJ1-50A, CommScope, Hickory, NC, United States) were employed, and the route of the cables was carefully arranged to reduce the noise. Since the higher frequency part of the EMP noise was visible from the waveform, it was used as an indicator while optimizing the route. The obtained ICT signals did not contain high frequency spikes.

The direct hit of the laser pulse or e-beam onto the ICT can potentially create secondary electrons and/or ionize the material, possibly contributing to the noise. The laser pulse was separated from e-beams to prevent it from hitting the ICT. An aperture was utilized for e-beam transverse size to be smaller than the acceptances of the ICT and Lanex, assuring that the e-beams did not hit the ICT or vacuum tube. The ICT was installed outside of the vacuum tube over a ceramic gap so that e-beams propagate in vacuum with minimum disturbance.

The low energy electrons could cause a large discrepancy between the ICT and Lanex measurements because of the following reasons. (1) Non-linear beam size evolution due to the space charge effect can lead to the acceptance mis-match between the two diagnostics. (2) The response of the Lanex against low energy electrons ( $< 1$  MeV) is not

clear. In this experiment, the ICT was installed 4.2 m away from the interaction point to assure that the low energy electrons diverge enough to minimize their contribution. Furthermore, the small residual magnetic field ( $< 0.4$  mT) of the magnetic spectrometer, and absorptions/scatterings at the foils used for the laser beam separation may have contributed to eliminate low energy electrons. The distance between ICT and Lanex was kept at a minimum to avoid acceptance mismatch.

Although no quantitative evaluation was performed for each noise source, it was considered to be critical to provide a low-noise environment for the charge measurement. Note that the accuracy of the measurement can be improved by a more sensitive camera for Lanex measurements, and by more sensitive electronics for ICT measurements.

### SUMMARY

A comprehensive study of the charge diagnostics for LPA produced e-beams was conducted. The cross-calibration between the Lanex and the activation-based charge diagnostic showed good agreement within the error of each diagnostic. The cross-calibration between the Lanex and the ICT showed good agreement as well. The result of the cross-calibrations can be summarized as follows,  $Q_{Act} = 93_{87}^{98}$ ,  $Q_{Lnx} = 100_{97}^{103}$ ,  $Q_{ICT} = 108_{100}^{116}$ , where they are normalized to the Lanex result, and super and sub scripts show result  $\pm$  the error of each diagnostics. The study showed that the all diagnostics can provide accurate charge measurement for LPA produced e-beams. The guideline for accurate measurements with the ICT under the harsh LPA environment was discussed, providing essential information for precise charge measurements of LPA produced e-beams.

### REFERENCES

- [1] E. Esarey, et al., *Rev. Mod. Phys.*, **81**, 1229 (2009).
- [2] W. P. Leemans, et al., *Nature Physics*, **2**, 696 (2006).
- [3] K. Nakamura, et al., *Phys. Plasmas*, **14**, 056708 (2007).
- [4] A. J. Gonsalves, et al., *Phys. Rev. Lett.*, **98**, 025002 (2007).
- [5] W. P. Leemans, et al., *Phys. Rev. Lett.*, **91**, 074802 (2003).
- [6] S. Kneip, et al., *Phys. Rev. Lett.*, **100**, 105006 (2008).
- [7] K. B. Unser, *Proc. of 89 Particle Accelerator Conference*, 71 (1989).
- [8] C. E. Clayton, et al., *Phys. Plasmas*, **1**, 1753 (1994).
- [9] C. Gahn, et al., *Rev. Sci. Instrum.*, **71**, 1642 (2000).
- [10] W. P. Leemans, et al., *Phys. Plasmas*, **8**, 2510 (2001).
- [11] Y. Glinec, et al., *Rev. Sci. Instrum.*, **77**, 103301 (2006).
- [12] A. Buck, et al., *Rev. Sci. Instrum.*, **81**, 033301 (2010).
- [13] S. Masuda, et al., *Rev. Sci. Instrum.*, **79**, 083301 (2008).
- [14] K. Nakamura, et al., submitted.
- [15] K. Zeil, et al., *Rev. Sci. Instrum.*, **81**, 013307 (2010).
- [16] B. Hidding, et al., *Rev. Sci. Instrum.*, **78**, 083301 (2007).
- [17] K. Nakamura, et al., *Rev. Sci. Instrum.*, **79**, 053301 (2008).
- [18] D. Pelowitz et al., *LA-UR-09-04150* (2009).